Biochemical Characterization of UDP-GlcNAc/Glc 4-Epimerase from *Escherichia coli* O86:B7†

Hongjie Guo,[#,‡] Lei Li,[§,‡] and Peng George Wang*[,#,§]

Department of Biochemistry and Chemistry, The Ohio State University, Columbus, Ohio 43210, and The State Key Laboratory of Microbial Technology, School of Life Science, Shandong University, Jinan, Shandong 250100, People's Republic of China

Received June 26, 2006; Revised Manuscript Received September 26, 2006

ABSTRACT: The O-antigen of lipopolysaccharide in Gram-negative bacteria plays an important role in bacterium−host interactions. *Escherichia coli* O86:B7 O-unit contains five sugar residues: one fucose (Fuc) and two each of *N*-acetylgalactosamine (GalNAc) and galactose (Gal). The entire O-antigen gene cluster was previously sequenced: *orf*1 was assigned the *gne* gene for the biosynthesis of UDP-GalNAc. To confirm this annotation, overexpression, purification, and biochemical characterization of Gne were performed. By using capillary electrophoresis, we showed that Gne can catalyze the interconversion of both UDP-GlcNAc/GalNAc and UDP-Glc/Gal almost equally well. The K_m values of Gne for UDP-Glc, UDP-Gal, UDP-GlcNAc, and UDP-GalNAc are 370, 295, 323, and 373 μM, respectively. The comparison of kinetic parameters of Gne from *Escherichia coli* O86:B7 to those of other characterized UDP-GlcNAc/Glc 4-epimerases indicated that it has relaxed specificity toward the four substrates, the first characterized enzyme to have this activity in the O-antigen biosynthesis. Moreover, the calculated k_{cat}/K_m values for UDP-GalNAc and UDP-Gal are approximately 2−4 times higher than those for UDP-GlcNAc and UDP-Glc, suggesting that Gne is slightly more efficient for the epimerization of UDP-GalNAc and UDP-Gal. One mutation (S306Y) resulted in a loss of epimerase activity for non-acetylated substrates by about 5-fold but totally abolished the activity for N-acetylated substrates, indicating that residue S^{306} plays an important role in the determination of substrate specificity.

Lipopolysaccharide (LPS)[1] is one of the major structural and immunodominant components in the outer membrane of Gram-negative bacteria. It typically contains three structural parts: lipid A (endotoxin), core oligosaccharide, and O-antigen (*1*−*3*). O-antigen is the most variable part in LPS (*3*−*6*). In *Escherichia coli* (including *Shigella*), 186 O serotypes have been recognized (*7*). Heteropolymeric O-antigen consists of many repeats of O-units (2−6 sugars per O-unit). The biosynthesis of the O-unit involves transfer of the first sugar residue from the UDP, GDP, CDP, or TDP (NDP) sugar precursor to the carrier lipid, undecaprenol-phosphate (UndP), followed by sequential transfer of other sugar residues from respective NDP sugar precursors by specific glycosyltransferases. The O-units are then translocated to the periplasmic side of the membrane by the O-unit flippase Wzx, and polymerized by Wzy to form the long chain O-antigen. Finally, the extended O-chain is ligated to the preformed lipid A/core by ligase WaaL (*8*−*10*). In *E. coli*, the O-antigen gene cluster lies between the *galF* and *gnd* genes in the chromosome (*11*).

The O-unit of *E. coli* O86:B7 contains five sugar residues: one fucose (Fuc) and two each of GalNAc and Gal (*12*). Previously, we determined the O-antigen gene cluster of O86:B7 (GenBank accession number AY220982) (*13*). Since the enzyme responsible for the synthesis of the UDP-Gal is a ubiquitous and obligatory enzyme in galactose metabolism, it is not duplicated in the O-antigen gene cluster (*8*). Only genes for the biosynthesis of precursors of GalNAc and Fuc are expected in the O-antigen gene cluster. On the basis of sequence similarity, we tentatively assigned *orf1* as the *gne* gene for the biosynthesis of UDP-GalNAc. However, direct biochemical evidence to confirm this annotation still needs to be found.

Gne from *E. coli* O86:B7 shares high similarity with many UDP-GlcNAc/Glc 4-epimerases, members of which can be divided into three groups based on their substrate specificity (*14*). Group 1 epimerases strongly prefer non-acetylated substrates (UDP-Glc/Gal), such as GalE from *E. coli* (eGalE). Group 2 epimerases such as GalE from human (hGalE) can epimerize both acetylated (UDP-GlcNAc/GalNAc) and non-acetylated substrates almost equally well. Group 3 includes WbgU from *P. shigelloides* and WbpP from *P. aeruginosa*, which show a strong preference for acetylated substrates.

Within the last 10 years, crystal structures for hGalE, eGalE, and WbpP have been solved at high resolution (*15*−*17*). Although epimerases from different sources differ significantly in size and quaternary structure, they share an identical mechanism of reaction, involving abstraction of a

† This work was supported from an endowed professorship of Ohio Eminent Scholar on macromolecular structure and function in the Department of Biochemistry at The Ohio State University.

* Corresponding author. Tel: 614-292-9884; fax: 614-292-3106; e-mail: wang.892@osu.edu.

[#] The Ohio State University.

[§] Shandong University.

[‡] Contributed equally to this work.

[1] Abbreviations: LPS, lipopolysaccharide; NDP, UDP, GDP, CDP, or TDP; uridine diphosphate; GlcNAc, *N*-acetylglucosamine; GalNAc, *N*-acetylgalactosamine; Gal, galactose; Glc, glucose; UndP, undecaprenol-phosphate; SDR, short-chain dehydrogenase/reductase; CE, capillary electrophoresis; IPTG, isopropyl 1-thio-β-D-galactospyranoside.

10.1021/bi0612770 CCC: $33.50
Published on Web 11/01/2006

hydride from the C-4 position of the sugar nucleotide by NAD prior to formation of a transient enzyme·NADH·keto-substrate complex. The sugar moiety of this complex in turn rotates 180° and abstracts the same hydride, leading to a steroselective inversion of the OH group. More recent studies have examined the molecular basis for the substrate specificity. Several bacterial species possess more than one copy of UDP-GlcNAc/Glc 4-epimerases, such as *Yersinia enterocolitica* O8 (www.sanger.ac.uk/Projects/Y_enterocolitica) and *E. coli* O157:H7 (*18*). Some bacterial species such as *Haemophilus. influenzae* Rd and *Campylobacter jejuni* (*19*, *20*) have a single copy but are known to produce more than one sugar precursor.

UDP-GlcNAc/Glc 4-Epimerases belong to the short-chain dehydrogenase/reductase (SDR) superfamily, which has two characteristic signature sequences (*21*, *22*). One is GXX-GXXG, popularly known as the Rossman fold, located near the amino-terminal end of the enzyme and the cofactor-binding pocket. The other one is YXXXK, in which Y and K function to abstract the 4′-hydroxyl hydrogen from the sugar substrate. Members of SDR superfamily are widespread in nature and have been isolated from various sources including mammals, insects, and bacteria (*23*−*25*). It is problematic to assign the function of the gene mainly based on the sequence similarity especially in the case of SDR superfamily members. Hence, biochemical characterization of Gne from *E. coli* O86:B7 is necessary to prove the function of this gene without ambiguity. In this work, we provide the biochemical evidence that Gne from *E. coli* O86:B7 is a UDP-GlcNAc/Glc 4-epimerase that can catalyze the interconversion of UDP-GlcNAc/GalNAc and UDP-Glc/Gal almost equally well.

MATERIALS AND METHODS

Materials. All chemical reagents unless stated otherwise were from Sigma. Plasmid vector pET15b was purchased from Novagen (Madison, WI). PCR reagents and restriction enzymes were purchased from Invitrogen (Carlsbad, CA). The DNA purification kit and gel purification kit were purchased from Qiagen (Valencia, CA). The HisTrap affinity column (5 mL) and HiLoad_16/60_superdex 200 column were from Amersham Pharmacia Biotech (Piscataway, NJ). All kits or enzymes were used following the manufacturer's instruction.

Cloning and Overexpression of Gne in the pET System. The *gne* gene was PCR amplified from *E. coli* O86:B7 using primers 1 (5′-CCGCTCGAGATGGTAAAGGAG-GTTTATATG, *Xho*I site is underlined) and 2 (5′-TTTTT-TATATCCATTTGGATTG). The PCR product was digested with *Xho*I and subsequently cloned into the *Xho*I site of pET15b. The constructs obtained were checked by restriction analysis and DNA sequencing.

The construct was subsequently transformed into the expression strain BL21 (DE3) (Novagen) with ampicillin (100 μg/mL) selection. For protein expression, 1 L of LB containing ampicillin was grown at 37 °C until the OD_{600} reached 0.6 and then induced by 0.2 mM isopropyl 1-thio-β-D-galactospyranoside (IPTG) and grown for 20 h at 16 °C. Cells were harvested by centrifugation and stored at −80 °C until needed. Expression was monitored by SDS−PAGE analysis, with Coomassie Blue staining or Western immunoblot using the penta-His anti-histidine tag antibody as instructed by the manufacturer.

Purification of Gne by Chromatography. Gne was expressed with the N-terminal histidine tag. The cells were washed and resuspended in buffer A (500 mM NaCl, 20 mM Tris-HCl, pH 8.0, 5 mM imidazole, and 0.2 mM PMSF) and then broken by 10 min of sonication (100 W). Low-speed centrifugation (10000*g*, 10 min, 4 °C) was carried out to remove the cell debris and inclusion bodies. The supernatant was loaded onto a 5-mL HisTrap affinity column. The column was washed with 10 column volumes of buffer B (500 mM NaCl, 20 mM Tris-HCl, pH 8.0, and 50 mM imidazole). The target protein was eluted with buffer C (500 mM NaCl, 20 mM Tris-HCl, pH 8.0, and 500 mM imidazole). Fractions containing the purified enzymes were collected and dialyzed against buffer D (20 mM Tris-HCl, pH 8.0) with a 10 K molecular weight cutoff (Millipore, Bedford, MA). The purified enzyme was concentrated to 2 mg/mL with 50% glycerol and then stored at −20 °C.

Determination of the Oligomerization Status of Gne by Gel-Filtration Analysis. Purified Gne protein was loaded onto a HiLoad_16/60_superdex 200 column equilibrated with buffer D containing 100 mM NaCl. The chromatographic run was carried out in the same buffer at a flow rate of 0.5 mL/min at 4 °C using AKTA FPLC system (Amersham Biosciences). Fractions of 2.0 mL were collected. The column was calibrated by running a set of gel-filtration markers (Amersham Biosciences).

Construction of the Plasmid Containing S306Y Mutation. The plasmid containing the Gne S306Y was constructed using the QuikChange Site-Directed Mutagenesis kit (Stratagene, La Jolla, CA). The template used for mutagenesis was Gne-pET15b construct described above. The primers used for mutagenesis were designed as follows: GNESYF: 5′-GAGGGGGATGTTGCGGAG-TACTGGGCGTCTGCTGATTTG-3′ and GNESYR: 5′-CAAATCAGCAGACGCCCAGTACTCCGCAA-CATCCCCCTC-3′. The entire length of the gene was sequenced to verify the mutation and to allow elimination of the constructs with unwanted secondary mutations.

CD Analyses. CD spectra were recorded on an AVIV 62A DS spectropolarimeter at 15 °C. CD data were collected over a wavelength range of 190−250 nm in a 1.0-mm path length quartz cell with a resolution of 0.5 nm and a bandwidth of 1 nm. Final spectra were the sum of 10 scans accumulated and were baseline corrected. The samples were measured in 10 mM potassium phosphate (pH 7.0) at a concentration of 0.2 mg/mL. Spectra were smoothed using five-point fast Fourier transform filtering (Origin version 6.0, Microcal).

Enzymatic Assays of Gne. The reaction mixture consisted of 1 mM substrate (UDP-Glc, UDP-Gal, UDP-GlcNAc, or UDP-GalNAc) and varying amounts of freshly prepared enzyme in 20 mM Tris-HCl, pH 8.0 in a total volume of 50 μL. The reactions were performed at 37 °C for 20 min and were quenched by boiling for 5 min. Analysis was performed by capillary electrophoresis (CE) using Beckman Coulter P/ACE MDQ Capillary electrophoresis. CE conditions were as follows: 75 μm i.d. capillary (China), 25 KV/80 μA, 5 s vacuum injection, with monitoring at 262 nm and 25 mM sodium tetraborate running buffer, pH 9.4.

Determination of Physicochemical Properties of Gne: Temperature and pH Range. Temperature experiments were performed in 20 mM Tris-HCl, pH 8.0 in a total volume of 50 μL with 100 ng of Gne and 0.5 mM UDP-Gal. Activities

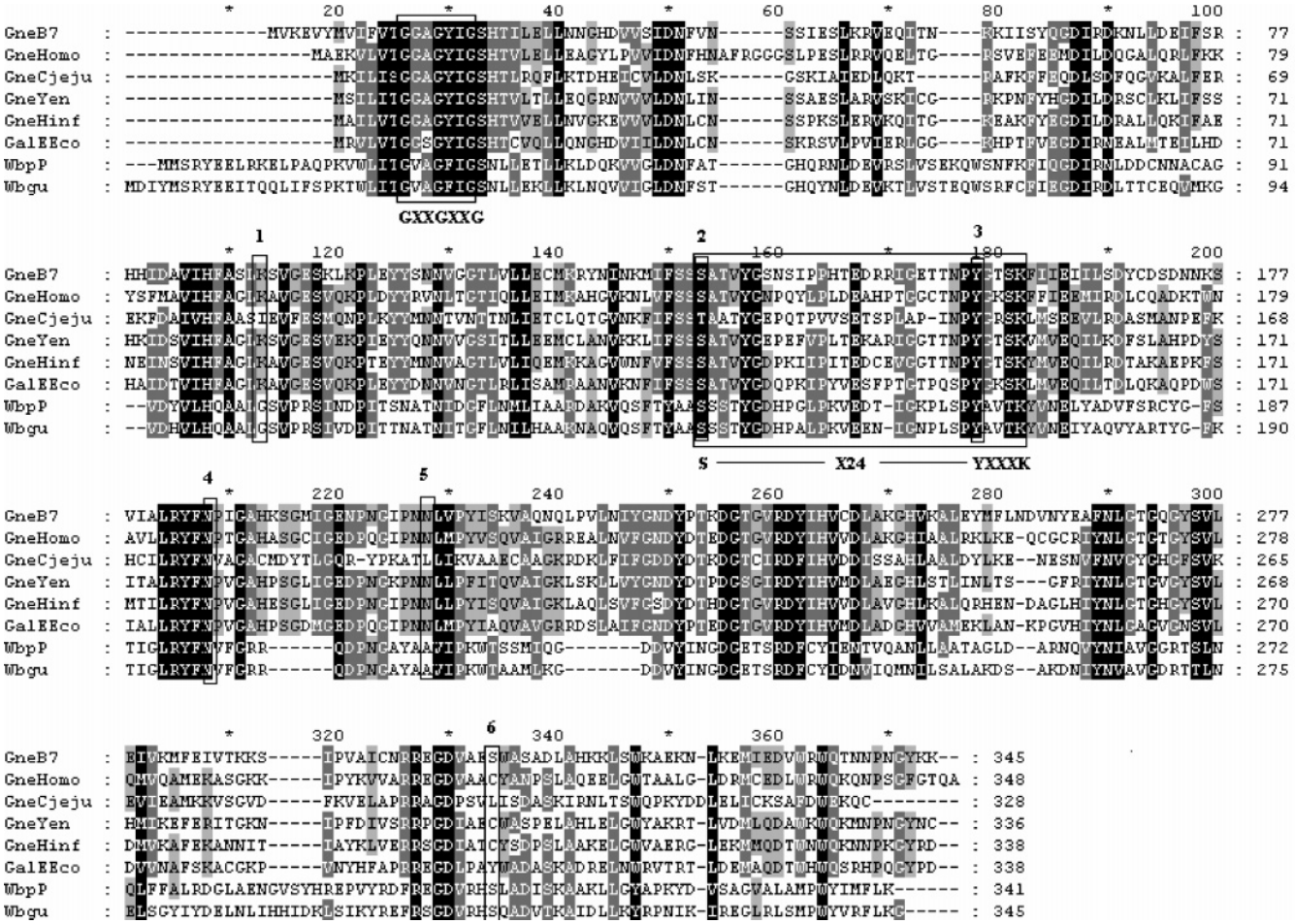

FIGURE 1: Multiple sequence alignment of Gne from *E. coli* O86:B7 with other UDP-GlcNAc/Glc 4-epimerases. GneB7 is Gne from *E. coli* O86:B7 characterized in this report. GneHomo, GneCjeju, GneYen, GneHinf, GalEEco, WbpP, and WbgU are epimerases from human, *C. jejuni*, *Y. enterocolitica* O8, *H. influenzae* Rd, *E. coli*, *P. aeruginosa*, and *P. shigelloides* O17. This alignment was made using ClustalX (*35*) and was reformatted in GeneDoc (http://www.psc.edu/biomed/genedoc/). The boxed aa residues are those of the predicted substrate-binding pocket.

were checked between 10 and 60 °C in 10 °C increments as well as 37 °C for 5 min. Activities of pH dependence were checked at 37 °C containing 0.5 mM UDP-Gal, 100 ng Gne, and varying pH buffer.

Determination of Kinetic Parameters of Gne for the Four Substrates. Reactions were conducted at 37 °C for 2 min in 20 mM Tris-HCl, pH 8.0 in a total volume of 50 μL. Substrate concentrations varied from 0.05 to 1.2 mM. The amounts of Gne used for UDP-Glc, UDP-Gal, UDP-GlcNAc, and UDP-GalNAc were 120, 40, 30, and 20 ng, respectively. The substrate concentrations used in the time course studies were 0.05 and 1.2 mM. The reactions were quenched at 0, 1, 2, 3, 5, 7, 10, and 15 min.

RESULTS

Sequence Analysis of Gne from E. coli O86:B7. The deduced protein sequence of *orf*1 in the O-antigen gene cluster of *E. coli* O86:B7 shares significant similarities with hGalE (66%), eGalE (65%), and other identified UDP-GlcNAc/Glc 4-epimerases. Thus, we putatively assigned it *gne*, which encoded the enzyme responsible for the conversion of UDP-GlcNAc to UDP-GalNAc. Gne also presented characteristic features of SDR superfamily. The first motif is $Gly^{13}-Xaa-Xaa-Gly^{16}-Xaa-Xaa-Gly^{19}$, located near the amino-terminal end of the enzyme. This motif is involved in the binding of the nucleotide cofactor to the domain (*21*). The second motif is $Ser^{130}-Xaa^{24}-Tyr^{155}-Xaa^{3}-Lys^{159}$, in which seryl, tyrosinyl, and lysyl residues are involved in the catalysis (Figure 1).

Protein Expression and Purification. Gne is a 38.8 kDa protein with a neutral isoelectric point (pI at 6.8). It was expressed as an N-terminal histidine-tagged protein in the pET system. Provided that the expression was carried out at low temperature (16 °C) with a low concentration of IPTG (0.2 mM), the target protein was expressed almost entirely in soluble form. Immobilized Ni affinity column was used to purify Gne, resulting in 80−90% pure proteins (Figure 2). On average, 30 mg of Gne could be obtained per liter of cell culture. The presence of the histidine tag was confirmed by Western immunoblot using an anti-histidine tag antibody (data not shown).

Gel filtration experiment was carried out to determine the molecular weight of Gne, generating a single peak indicative of a stable oligomeric complex. The elution volume corresponds to a molecular weight of 80 kDa, demonstrating that Gne exists as a dimer under the experimental conditions (data not shown). The result is in agreement with the determined structures of eGalE, hGalE, and WbpP, which all formed a homodimer (*15*, *26*, *27*).

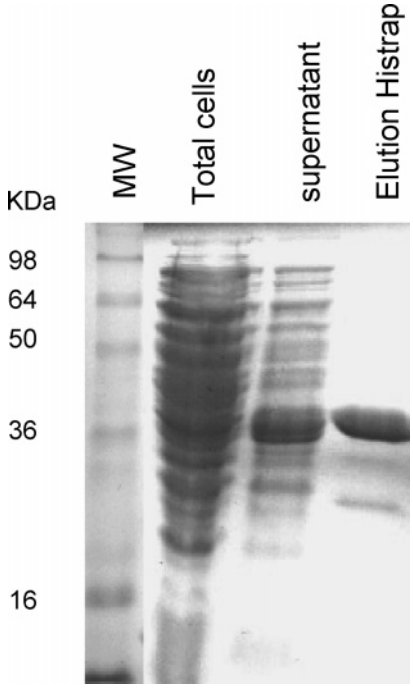

FIGURE 2: SDS−PAGE analysis of Gne expression and purification. The detection was performed with Coomassie Blue staining.

Characterization of Gne Activity by Capillary Electrophoresis (CE). CE was used to characterize the enzymatic activities of Gne. It can identify the reaction products by comparison to the standard compounds. The epimers could be baseline-resolved with 9.5, 10.0, 9.2, and 9.7 min retention times for UDP-Glc, UDP-Gal, UDP-GlcNAc, and UDP-GalNAc, respectively (Figures 3 and 4). The results showed that Gne can catalyze the interconversion of both UDP-Glc/Gal and UDP-GlcNAc/GalNAc. The epimerization reaction between UDP-Glc and UDP-Gal, when complete, consistently resulted in a 3:1 ratio of UDP-Glc to UDP-Gal, irrespective of the initial substrate (Figure 3). The epimerization between UDP-GlcNAc and UDP-GalNAc resulted in a 2.6:1 ratio of UDP-GlcNAc to UDP-GalNAc irrespective of the initial substrate (Figure 4).

Biophysical Properties of Gne. Gne exhibits the highest activity at 37 °C and is active in a wide temperature range (from 10 to 40 °C) (data not shown). The enzyme also exhibited activity in a very broad pH range with the highest activity between pH 7.0 and 9.0 (data not shown).

Determination of the Kinetic Parameters. Time course experiments performed with different enzyme dilutions indicated that the rate of conversion of UDP-Glc is much slower than that of UDP-Gal at equal enzyme dilution (Figure 5A). The rate of conversion of UDP-GlcNAc is slower than that of UDP-GalNAc too (Figure 5B). To ensure initial rate conditions, enzyme dilutions were selected such that substrate conversion of 10% or less was achieved after a 2-min reaction. The K_m and V_{max} parameters of Gne were determined under these initial rates conditions (Table 1 and Figure 6). The K_m values for UDP-Glc, UDP-Gal, UDP-GlcNAc, and UDP-GalNAc are 370, 295, 323, and 373 μM, respectively. Gne showed approximately the same affinity for the four substrates. The calculated k_{cat}/K_m values for UDP-GalNAc and UDP-Gal are approximately 2−4 times higher

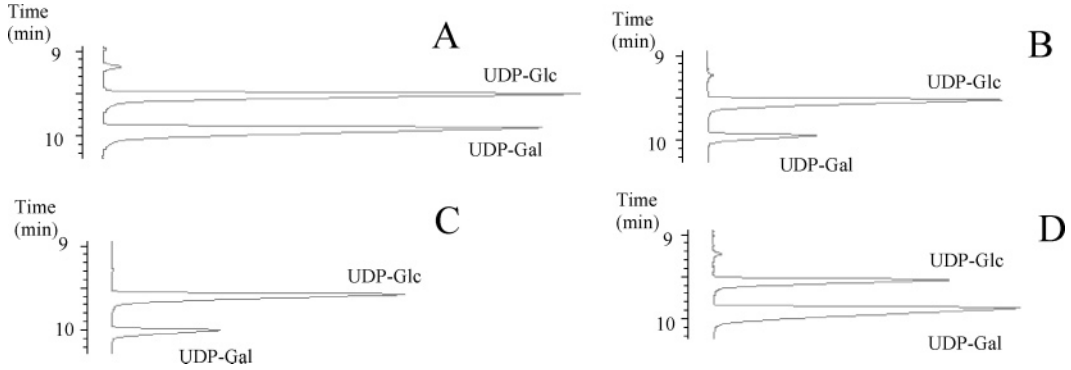

FIGURE 3: Capillary electrophoresis traces of the UDP-Glc and UDP-Gal reaction after reaching equilibrium. (A) Standard mixture of UDP-Glc and UDP-Gal, 1 mM each; (B) UDP-Glc reaction; (C) UDP-Gal reaction; (D) spiked UDP-Glc reaction (0.5 mM UDP-Gal added after quenching). In each case, the UDP-sugar substrate was used at 1 mM. UDP-Glc has a retention time of 9.5 ± 0.1 min, and UDP-Gal has a retention time of 10.0 ± 0.1 min.

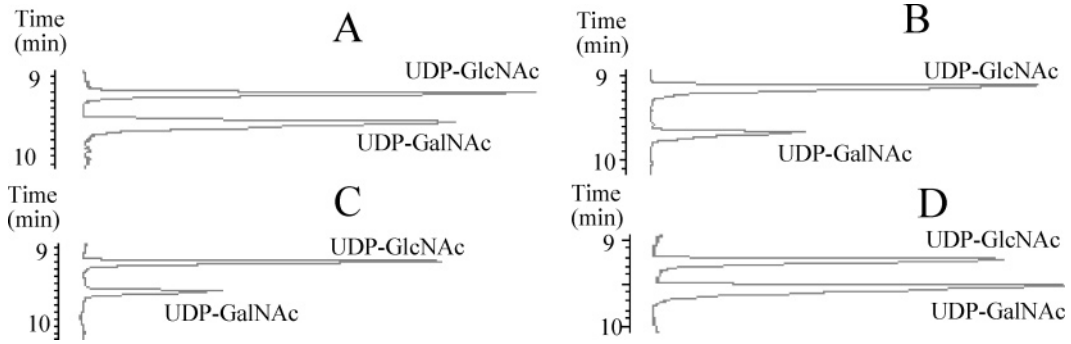

FIGURE 4: Capillary electrophoresis traces of the UDP-GlcNAc and UDP-GalNAc reaction after reaching equilibrium. (A) UDP-GlcNAc and UDP-GalNAc standard, 1 mM each; (B) UDP-GlcNAc reaction; (C) UDP-GalNAc reaction; (D) spiked UDP-GlcNAc reaction (0.5 mM UDP-GalNAc added after quenching). In each case, the UDP-sugar substrate was used at 1 mM. UDP-GlcNAc has a retention time of 9.2 ± 0.1 min, and UDP-GalNAc has a retention time of 9.7 ± 0.1 min.

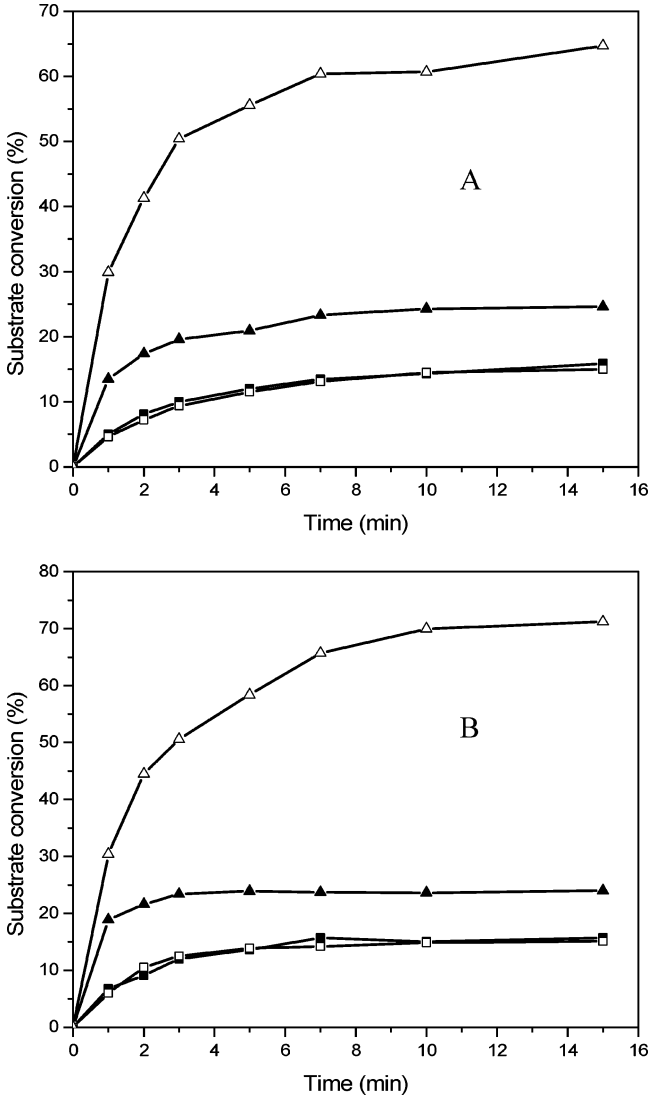

FIGURE 5: Time course for the epimerization of UDP-Glc/Gal by Gne using capillary electrophoresis (A). Reactions consisted of 0.05 mM substrate (triangles) and 1.2 mM substrate (squares). UDP-Gal, open symbols; UDP-Glc, solid symbols. The amounts of enzyme used were 210 and 70 ng for UDP-Glc and UDP-Gal, respectively. Time course for the epimerization of UDP-GlcNAc/GalNAc by Gne using capillary electrophoresis (B). Reactions consisted of 0.05 mM substrate (triangles) and 1.2 mM substrate (squares). UDP-GalNAc, open symbols; UDP-GlcNAc, solid symbols. The amounts of enzyme used were 45 and 30 ng for UDP-GlcNAc and UDP-GalNAc, respectively.

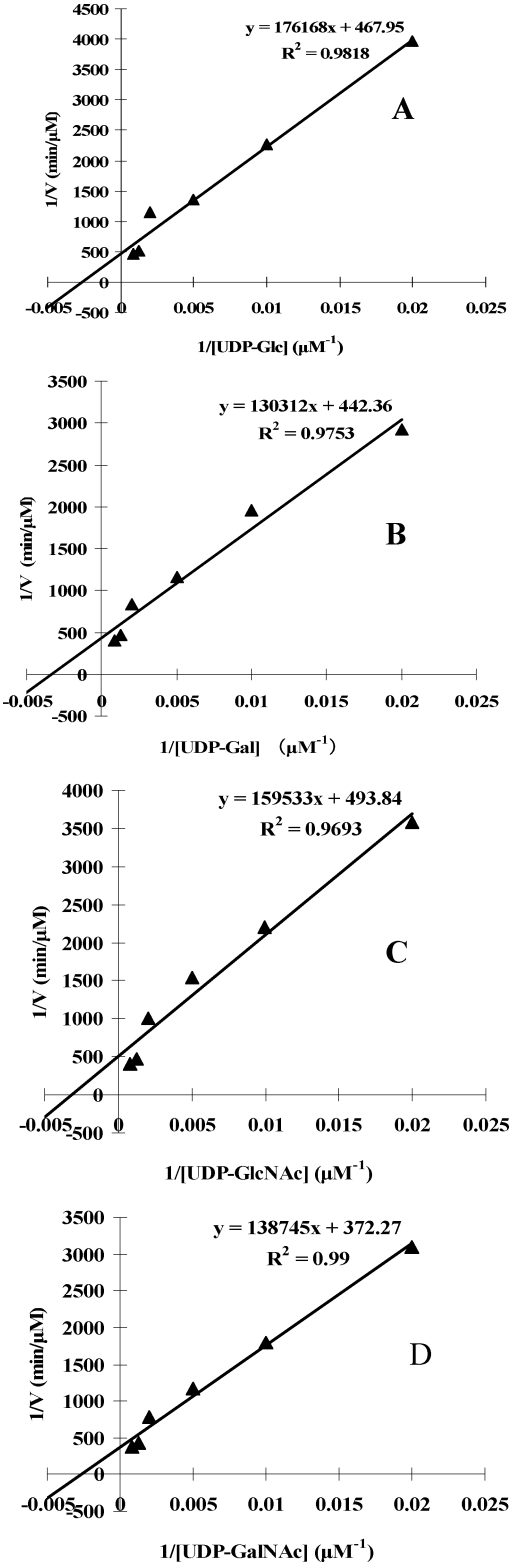

FIGURE 6: Lineweaver−Burk plot for Gne from *E. coli* O86:B7 toward UDP-Glc (A), UDP-Gal (B), UDP-GlcNAc (C), and UDP-GalNAc (D). Double reciprocal plot was constructed by plotting $1/V$ against $1/S$ analyzed over a range of substrate concentrations (0.05−1.2 mM). The plot represents the means of three experiments.

than those for UDP-GlcNAc and UDP-Glc, indicating that Gne is slightly more efficient for the epimerization of UDP-GalNAc and UDP-Gal.

Functional Role of S^{306} in Gne. Crystal structures are now available for all the three different groups of UDP-GlcNAc/Glc 4-epimerases, including eGalE, hGalE, and WbpP. A comprehensive analysis of the relationship between sequences, three-dimensional (3D) structure, and the substrate specificity has led to an abstract model to facilitate a better understanding of the interactions between the enzyme and its substrate in the binding pocket (*15*, *28*). In this model, the substrate binding pocket can be viewed as a hexagonal-shaped box in which the bottom is formed by the nicotinamide ring of the cofactor, and six walls are formed by different regions of the enzymes. Three of the six walls are composed of highly conserved amino acids: S, Y, and N, the first two are also part of SYK catalytic triad. The remaining three walls vary between group 1, 2, and 3 UDP-GlcNAc/Glc 4-epimerases.

We showed above that Gne is able to catalyze the interconversion of UDP-GalNAc and UDP-GlcNAc, and in addition, the interconversion of UDP-Gal and UDP-Glc

Table 1: Kinetic Parameters of Gne and S306Y-Gne Compared with Other Characterized Epimerases

substrate	enzyme	K_m (μM)	V_{max} (μmol/min)	enzyme (pmol/assay)	k_{cat} (min^{-1})	k_{cat}/K_m (min^{-1} × mM^{-1})
UDP-GlcNAc	GneB7[a]	323	2.0×10^{-3}	0.375	5400	16718
	GneCje[b]	1087	63.2	0.083	4938	4530
	WbpP[c]	224	7.4×10^{-4}	6.2	120	536
	WbgU[d]	137	1.7×10^{-3}	3.7	461	3443
UDP-GalNAc	Gne_{B7}	373	2.7×10^{-3}	0.25	10744	28804
	Gne_{Cje}	1070	190.4	0.083	14875	13902
	WbpP	197	8.4×10^{-4}	3.1	271	1375
	WbgU	131	1.9×10^{-3}	1.85	1038	7924
UDP-Glc	Gne_{B7}	370	2.1×10^{-3}	1.5	1402	3786
	S306Y-Gne[e]	619	3.3×10^{-3}	7.5	444	717
	Gne_{Cje}	780	56.8	0.083	4437	5688
	WbpP	237	5.4×10^{-5}	436	0.124	0.523
	WbgU	153	1.7×10^{-4}	740	0.226	1.78
UDP-Gal	Gne_{B7}	295	2.3×10^{-3}	0.5	4522	15328
	S306Y-Gne	607	3.4×10^{-3}	2.5	1368	2253
	Gne_{Cje}	784	222.8	0.083	17406	22202
	WbpP	251	8.2×10^{-5}	436	0.188	0.749
	WbgU	160	4.6×10^{-4}	740	0.615	3.83
	eGalE[f]	225	N/R	N/R	45600	202667

[a] Gne_{B7} is characterized in this report. [b] Data from *C. jejuni* (see ref 14). [c] Data from *P. aeruginosa* O6 (see ref 29). [d] Data from *P. shigelloides* (see ref 30). [e] S306Y-Gne is characterized in this report. [f] Data from *E. coli* (see ref 14).

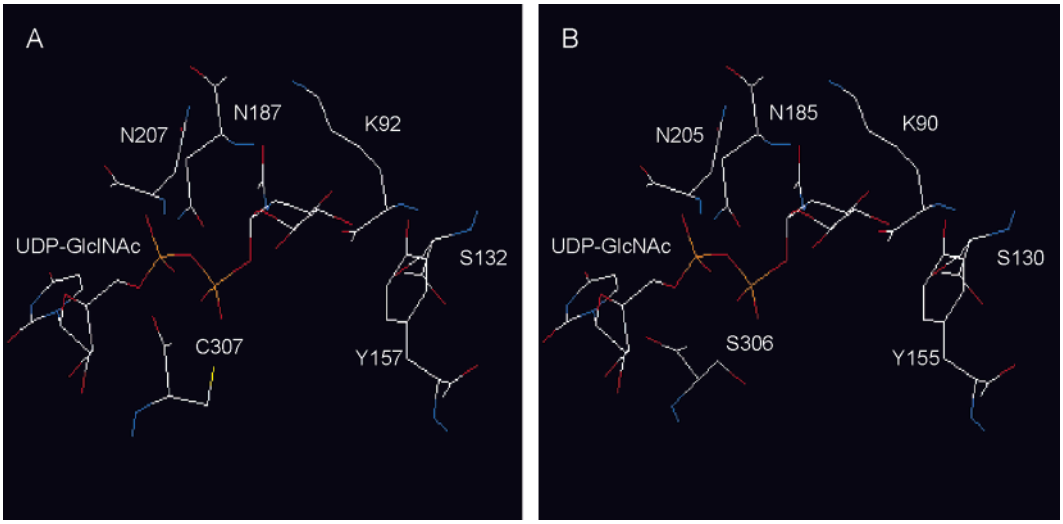

FIGURE 7: Molecular modeling of the active sites of hGalE (A) and Gne from O86:B7 (B). Only one amino acid difference was found in the sugar binding pockets between hGalE and Gne from O86:B7. When the residue Cys307 (A) was replaced with Ser306 (B), the cavity is still large enough to accommodate the aminoacetyl group of UDP-GlcNAc.

almost at equal efficiency, so it should be classified in the same group with hGalE. To elucidate the molecular basis behind this substrate specificity, we constructed the structural model of Gne based on the crystal structure of hGalE. A reliable model could be obtained due to the high degree of identity between Gne and hGalE. Similar to that of hGalE, the overall structure of Gne consists of two distinct domains. The N-terminal domain consists of a seven-stranded parallel β-sheet flanked on either side by α-helices. The C-terminal domain is composed of five strands of β-sheet and four α-helices.

In the active site model, the six amino acid residues that make up the UDP sugar-binding pocket of Gne are K^{90}, S^{130}, Y^{155}, N^{185}, N^{205}, and S^{306} (Figure 1, residues numbered 1−6 in Figure 1). Comparison of the substrate binding pockets between Gne and hGalE revealed only a single amino acid residue difference: S^{306} in Gne vs C^{307} in hGalE. Serine and cysteine share similar bulk; thus, the substitution of cysteine for serine would have a minor effect on the size of sugar pocket (Figure 7); therefore, the substrate pocket in Gne is large enough to accommodate the aminoacetyl group of the substrate. However, the corresponding residue in eGalE (a genuine UDP-Glc/Gal 4-epimerse) is a much bulkier Y^{299}, which significantly reduced the size of the pocket, resulting in the exclusion of the aminoacetyl group in the eGalE complex structure.

To elucidate the role of S^{306} as a determinant of substrate specificity in Gne, site-directed mutagenesis of Gne was constructed. We substituted the bulky residue tyrosine in place of the natural serine. The resultant S306Y-Gne allele was expressed and purified as described for the wild-type Gne. Finally, in vitro activity assays were performed using either UDP-Gal or UDP-GalNAc as the substrate. The result clearly demonstrated that S306Y mutation totally abolished activity toward the acetylated substrate (data not shown). To elucidate the effect of the mutation on the non-acetylated substrates, kinetic parameters of S306Y-Gne for UDP-Glc and UDP-Gal were determined (Table 1). The calculated k_{cat}/K_m values of S3006Y-Gne for UDP-Glc and UDP-Gal are approximately 5-fold less than those of the wild-type enzyme,

suggesting that the mutation might have a subtle effect on the overall protein conformation, thereby affecting the enzyme activity. A single mutation S306Y resulted in a switch of Gne from group 2 to group 1 UDP-GlcNAc/Glc 4-epimerase.

DISCUSSION

Most of the sugars in O-antigen are transferred from nucleotide sugar precursors. Some common sugar nucleotides such as UDP-Glc, UDP-Gal, and UDP-GlcNAc are also present in other pathways; their biosynthetic genes are located outside the O-antigen gene cluster (*8*). eGalE (EC 5.1.3.2), a ubiquitous enzyme responsible for the biosynthesis of UDP-Gal, was also identified in *E. coli* O86:B7 (unpublished data). eGalE belongs to group 1 UDP-GlcNAc/Glc 4-epimerase and cannot accept acetylated substrates. Hence, *E. coli* O86:B7 needs an additional UDP-GlcNAc 4-epimerase (often called Gne for UDP-Glc*N*Ac 4-*e*pimerase) for the biosynthesis of UDP-GalNAc. The evidence presented in this work conclusively demonstrated that the previously annotated *gne* gene encodes a UDP-GlcNAc/Glc 4-epimerase that can catalyze the interconversion of UDP-GlcNAc/GalNAc and UDP-Glc/Gal almost equally well. This is the first characterized UDP-GlcNAc/Glc 4-epimerase showing such activity in the O-antigen gene cluster. The other three characterized UDP-GlcNAc/Glc 4-epimerases from O-antigen gene cluster are WbpP, WbgU, and Gne from *Y. enterocolitica* O8. They all belong to group 3 epimeriases, showing strong preference for acetylated substrates (*29*−*31*). Provided that this is a very important group of enzymes involved in the O-antigen biosynthesis, therefore, understanding the molecular basis for substrate specificity might lead to the development of novel therapeutic agents useful to modulate the activity of the epimerases as needed.

The kinetic characterization of Gne was performed to assess its substrate specificity. The K_m values of the purified Gne for the four substrates (UDP-Glc, UDP-Gal, UDP-GlcNAc, and UDP-GalNAc) are very close to one another. The k_{cat}/K_m values for UDP-GalNAc and UDP-GlcNAc are only about 2−4 times higher than those for UDP-Gal and UDP-Glc. Compared with the kinetic parameters of other two characterized epimerases WbpP and WbgU from group 3, which exhibit similar K_m values for the four substrates but show about 1000-fold lower of k_{cat}/K_m values for non-acetylated substrates than for acetylated substrates (Table 1), our results strongly demonstrated that Gne from *E. coli* O86:B7 can catalyze the interconversion of UDP-GlcNAc/GalNAc and UDP-Glc/Gal almost equally well. It is the third member in group 2 UDP-GlcNAc/Glc 4-epimerase reported until now. The other two enzymes in the same group are hGalE and Gne from *C. jejuni*.

There are several reported examples of UDP-GlcNAc/Glc 4-epimerase showing activity toward all the four substrates. However, they generally display much more preference for one set of substrates over the other. For example, WbpP, WbgU, and Gne from *Y. enterocolitica* O8 can epimerize both acetylated and nonacetylated substrates, but the efficiency of interconversion of nonacetylated substrates is very low (*29*−*31*). Thus, these three enzymes are classified in group 3. Another example is Gne from *Bacillus subtilis*, which can catalyze UDP-glucose as well as UDP-GlcNAc 4-epimerization, but it is much more efficient in catalyzing the interconversion between nonacetylated substrates than between the corresponding acetylated substrates. As a result, it is classified in group 1. In our work, Gne from O86:B7 is able to catalyze both sets of substrates almost at equal efficiency, so it is classified in group 2.

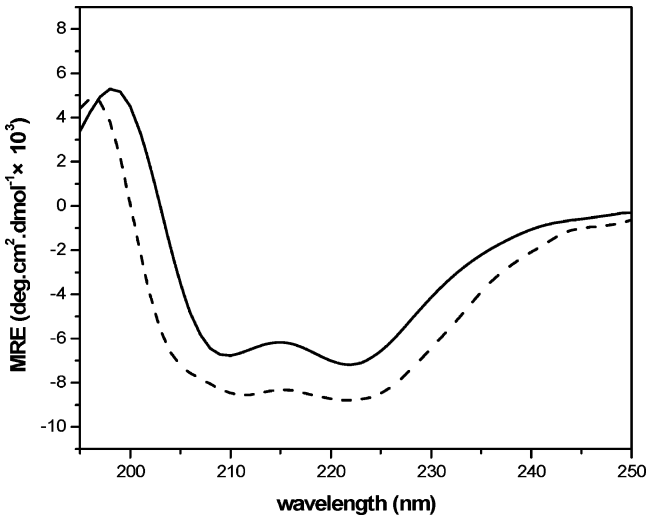

FIGURE 8: Far-UV circular dichroism analysis of Gne wild type (solid) and S306Y mutant (dash).

The molecular basis for the substrate specificity in epimerases is an important question to address. Structural and mutational studies led to a structural model implicating a limited number of residues to explain the substrate specificity. In this model, the substrate-binding pocket can be viewed as a hexagonal-shaped box. On the basis of this model, it was hypothesized that widening the binding pocket would allow catalysis of both types of substrates, while narrowing it would result in limitation to only nonacetylated substrates. Two previously reported results of C307Y mutant in hGalE and C297Y mutant in Gne from *Y. enterocolitica* O8 support this simple hypothesis (*31*, *32*), showing that narrowing the substrate binding pocket resulted in a significant loss of activity with acetylated substrates, but has no effect on nonacetylated substrates. However, other two data concerning Y299C mutation in eGalE and S306Y mutation in WbpP showed contrary results. The mutation in eGalE resulted in loss of catalysis of nonacetylated substrates, and the mutation in WbpP totally abolished the activity with regard to all substrates (*15*, *17*). Thus, prediction of substrate specificity solely based on sequence analysis might lead to incorrect functional assignments. It is necessary to determine the role of residue Ser^{306} in the determination of substrate specificity. Gne from B7 shared same substrate specificity with hGalE; previous data left open the question of whether the same rationale could govern substrate selectivity in Gne from B7. Our results showed that S306Y-Gne mutant totally abolished the activity on bulky substrate (UDP-GalNAc). Contrary to hGalE, it also demonstrated an almost 5-fold loss of activity with regard to interconversion of UDP-Gal/UDP-Glc. This is the first example where narrowing the substrate binding pocket not only abolishes the activity toward acetylated substrates but also results in a loss of activity toward nonacetylated substrates. CD spectra were recorded to assess whether this mutation had altered global protein folding. The differences between the CD spectra of

the S306Y mutant with that of the wild type were subtle and could simply reflect a limited change in the global protein folding (Figure 8). Furthermore, if the mutation resulted in the global perturbation of the protein structure, it would abolish activity on all substrates and not specifically on one. The S306Y mutant still retained the activity on nonacetylated substrate but at a reduced rate, suggesting that the mutation resulted in a subtle structural change. The results above strongly suggested that the loss of activity on the epimerization of acetylated substrate was not caused by the significant protein secondary or tertiary structure changes but by the change of the size of the sugar binding pocket.

In summary, we have demonstrated that Gne from *E. coli* O86:B7 can catalyze the interconversion of UDP-GlcNAc/GalNAc and UDP-Glc/Gal almost equally well. This is the first characterized epimerase to have this activity in the O-antigen biosynthesis. Considering the essential roles of the GalE/Gne enzymes in maintaining viability and /or virulence of major pathogens (*33*, *34*), exploring the molecular basis for the substrate specificity is not only important in the basic science but also has clinical significance. Our study showed the first example where narrowing the binding pocket not only abolished the activity toward acetylated substrates but also reduced the activity toward nonacetylated substrates. Hence, this report cautions against hasty functional assignments based solely on sequence alignment in the absence of biochemical data.

ACKNOWLEDGMENT

P.G.W. acknowledges the support from an endowed professorship of Ohio Eminent Scholar on macromolecular structure and function in the Department of Biochemistry at The Ohio State University.

REFERENCES

1. Raetz, C. R., and Whitfield, C. (2002) Lipopolysaccharide endotoxins, *Annu. Rev. Biochem. 71*, 635−700.
2. Raetz, C. R. (1990) Biochemistry of endotoxins, *Annu. Rev. Biochem. 59*, 129−170.
3. Reeves, P. P., and Wang, L. (2002) Genomic organization of LPS-specific loci, *Curr. Top. Microbiol. Immunol. 264*, 109−135.
4. Reeves, P. (1995) Role of O-antigen variation in the immune response, *Trends Microbiol. 3*, 381−386.
5. Lerouge, I., and Vanderleyden, J. (2002) O-antigen structural variation: mechanisms and possible roles in animal/plant-microbe interactions, *FEMS Microbiol. Rev. 26*, 17−47.
6. Wang, L., Andrianopoulos, K., Liu, D., Popoff, M. Y., and Reeves, P. R. (2002) Extensive variation in the O-antigen gene cluster within one Salmonella enterica serogroup reveals an unexpected complex history, *J. Bacteriol. 184*, 1669−1677.
7. Guo, H., Kong, Q., Cheng, J., Wang, L., and Feng, L. (2005) Characterization of the Escherichia coli O59 and O155 O-antigen gene clusters: The atypical wzx genes are evolutionary related, *FEMS Microbiol. Lett. 248*, 153−161.
8. Samuel, G., and Reeves, P. (2003) Biosynthesis of O-antigens: genes and pathways involved in nucleotide sugar precursor synthesis and O-antigen assembly, *Carbohydr. Res. 338*, 2503−2519.
9. Whitfield, C. (1995) Biosynthesis of lipopolysaccharide O antigens, *Trends Microbiol. 3*, 178−185.
10. Valvano, M. A. (2003) Export of O-specific lipopolysaccharide, *Front Biosci 8*, s452−471.
11. Guo, H., Feng, L., Tao, J., Zhang, C., and Wang, L. (2004) Identification of Escherichia coli O172 O-antigen gene cluster and development of a serogroup-specific PCR assay, *J. Appl. Microbiol. 97*, 181−190.
12. Yi, W., Bystricky, P., Yao, Q., Guo, H., Zhu, L., Li, H., Shen, J., Li, M., Ganguly, S., Bush, C. A., and Wang, P. G. (2005) Two different O-polysaccharides from *Escherichia coli* O86 are produced by different polymerization of the same O-repeating unit, *Carbohydr. Res. 341*, 100−108.
13. Guo, H., Yi, W., Shao, J., Lu, Y., Zhang, W., Song, J., and Wang, P. G. (2005) Molecular analysis of the O-antigen gene cluster of Escherichia coli O86:B7 and characterization of the chain length determinant gene (wzz), *Appl. Environ. Microbiol. 71*, 7995−8001.
14. Bernatchez, S., Szymanski, C. M., Ishiyama, N., Li, J., Jarrell, H. C., Lau, P. C., Berghuis, A. M., Young, N. M., and Wakarchuk, W. W. (2005) A single bifunctional UDP-GlcNAc/Glc 4-epimerase supports the synthesis of three cell surface glycoconjugates in Campylobacter jejuni, *J. Biol. Chem. 280*, 4792−4802.
15. Ishiyama, N., Creuzenet, C., Lam, J. S., and Berghuis, A. M. (2004) Crystal structure of WbpP, a genuine UDP-N-acetylglucosamine 4-epimerase from Pseudomonas aeruginosa: substrate specificity in UDP-hexose 4-epimerases, *J. Biol. Chem. 279*, 22635−22642.
16. Thoden, J. B., Wohlers, T. M., Fridovich-Keil, J. L., and Holden, H. M. (2000) Crystallographic evidence for Tyr 157 functioning as the active site base in human UDP-galactose 4-epimerase, *Biochemistry 39*, 5691−5701.
17. Thoden, J. B., Henderson, J. M., Fridovich-Keil, J. L., and Holden, H. M. (2002) Structural analysis of the Y299C mutant of Escherichia coli UDP-galactose 4-epimerase. Teaching an old dog new tricks, *J. Biol. Chem. 277*, 27528−27534.
18. Perna, T. P., Plunkett, G. I., etc, and Blattner, F. R. (2001) Genome sequence of enterhaemorrhagic *Escherichia coli* O157:H7, *Nature 409*, 529−533.
19. Risberg, A., Masoud, H., Martin, A., Richards, J. C., Moxon, E. R., and Schweda, E. K. (1999) Structural analysis of the lipopolysaccharide oligosaccharide epitopes expressed by a capsule-deficient strain of *Haemophilus influenzae* Rd, *Eur. J. Biochem. 261*, 171−180.
20. Parkhill, J., Wren, B. W., Mungall, K., Ketley, J. M., Churcher, C., Basham, D., Chillingworth, T., Davies, R. M., Feltwell, T., Holroyd, S., Jagels, K., Karlyshev, A. V., Moule, S., Pallen, M. J., Penn, C. W., Quail, M. A., Rajandream, M. A., Rutherford, K. M., van Vliet, A. H., Whitehead, S., and Barrell, B. G. (2000) The genome sequence of the food-borne pathogen Campylobacter jejuni reveals hypervariable sequences, *Nature 403*, 665−668.
21. Cho, H., Hamza, A., Zhan, C. G., and Tai, H. H. (2005) Key NAD+-binding residues in human 15-hydroxyprostaglandin dehydrogenase, *Arch. Biochem. Biophys. 433*, 447−453.
22. Hwang, C. C., Chang, Y. H., Hsu, C. N., Hsu, H. H., Li, C. W., and Pon, H. I. (2005) Mechanistic roles of Ser-114, Tyr-155, and Lys-159 in 3alpha-hydroxysteroid dehydrogenase/carbonyl reductase from Comamonas testosterone, *J. Biol. Chem. 280*, 3522−3228.
23. Matsunaga, T., Shintani, S., and Hara, A. (2006) Multiplicity of mammalian reductases for xenobiotic carbonyl compounds, *Drug Metab. Pharmacokinet. 21*, 1−18.
24. Vogan, E. M., Bellamacina, C., He, X., Liu, H. W., Ringe, D., and Petsko, G. A. (2004) Crystal structure at 1.8 Å resolution of CDP-D-glucose 4, 6-dehydratase from *Yersinia pseudotuberculosis*, *Biochemistry 43*, 3057−3067.
25. Liden, M., Tryggvason, K., and Eriksson, U. (2003) Structure and function of retinol dehydrogenases of the short chain dehydrogenase/reductase family, *Mol. Aspects Med. 24*, 403−409.
26. Thoden, J. B., Wohlers, T. M., Fridovich-Keil, J. L., and Holden, H. M. (2001) Human UDP-galactose 4-epimerase. Accommodation of UDP-N-acetylglucosamine within the active site, *J. Biol. Chem. 276*, 15131−15136.
27. Thoden, J. B., Frey, P. A., and Holden, H. M. (1996) High-resolution X-ray structure of UDP-galactose 4-epimerase complexed with UDP-phenol, *Protein Sci. 5*, 2149−2161.
28. Demendi, M., Ishiyama, N., Lam, J. S., Berghuis, A. M., and Creuzenet, C. (2005) Towards a better understanding of the substrate specificity of the UDP-*N*-acetylglucosamine C4 epimerase WbpP, *Biochem. J. 389*, 173−180.
29. Creuzenet, C., Belanger, M., Wakarchuk, W. W., and Lam, J. S. (2000) Expression, purification, and biochemical characterization of WbpP, a new UDP-GlcNAc C4 epimerase from Pseudomonas aeruginosa serotype O6, *J. Biol. Chem. 275*, 19060−19067.
30. Kowal, P., and Wang, P. G. (2002) New UDP-GlcNAc C4 epimerase involved in the biosynthesis of 2-acetamino-2-deoxy-L-altruronic acid in the O-antigen repeating units of *Plesiomonas shigelloides* O17, *Biochemistry 41*, 15410−15414.

31. Bengoechea, J. A., Pinta, E., Salminen, T., Oertelt, C., Holst, O., Radziejewska-Lebrecht, J., Piotrowska-Seget, Z., Venho, R., and Skurnik, M. (2002) Functional characterization of Gne (UDP-*N*-acetylglucosamine-4-epimerase), Wzz (chain length determinant), and Wzy (O-antigen polymerase) of *Yersinia enterocolitica* serotype O:8, *J. Bacteriol. 184*, 4277−4287.
32. Schulz, J. M., Watson, A. L., Sanders, R., Ross, K. L., Thoden, J. B., Holden, H. M., and Fridovich-Keil, J. L. (2004) Determinants of function and substrate specificity in human UDP-galactose 4′-epimerase, *J. Biol. Chem. 279*, 32796−32803.
33. Roper, J. R., Guther, M. L., Milne, K. G., and Ferguson, M. A. (2002) Galactose metabolism is essential for the African sleeping sickness parasite *Trypanosoma brucei*, *Proc. Natl. Acad. Sci.* U.S.A. *99*, 5884−5889.
34. Fry, B. N., Feng, S., Chen, Y. Y., Newell, D. G., Coloe, P. J., and Korolik, V. (2000) The galE gene of Campylobacter jejuni is involved in lipopolysaccharide synthesis and virulence, *Infect. Immun. 68*, 2594−2601.
35. Thompson, J. D., Gibson, T. J., Plewniak, F., Jeanmougin, F., and Higgins, D. G. (1997) The CLUSTAL_X windows interface: flexible strategies for multiple sequence alignment aided by quality analysis tools, *Nucleic Acids Res. 25*, 4876−4882.

BI0612770